Focal evolution induced by combination of nonspiral and spiral phase plates

Xiumin Gao (高秀敏) and Jian Wang (王 健)

Electronics and Information College, Hangzhou Dianzi University, Hangzhou 310018

Received September 5, 2006

Focusing properties of Gaussian beam induced by nonspiral and spiral phase plates are investigated numerically. The nonspiral phase plate introduces phase singularity to the incident beam, and the spiral one adjusts the radial phase distribution. Intensity distributions in geometrical focal plane show that the parameters of phase plates can alter the intensity distributions considerably. And local dark focal spots may be obtained, the focal spot may evolve into a circle, a two-peak spot, or a curve line, which indicates that the combination of nonspiral and spiral phase plates can be used to form novel focal spots.

OCIS codes: 350.5030, 230.0230, 220.1230.

Since 1970s, singular optics studying optical vortices has been growing rapidly for its interesting properties and promising applications[1−4]. Optical vortices can be used to construct highly versatile optical traps to trap and rotate particles[5,6]. Several methods have been proposed to construct optical vortex, including hologram[7], cylindrical lens mode converter[8], and phase plate[9]. In fact, phase plate has been proposed in many optical systems[10,11]. Phase plate can induce focal split[12] and alter optical trapping gradient force[13] and focal depth[14]. Kim *et al.* demonstrated that not only spiral phase plate but also nonspiral one can construct optical vortex beam[15]. They found that a linear phase variation on one half of a Gaussian beam can induce phase singularity, and showed some experimental far-field intensity distributions. Spiral phase plate can be used to alter wavefront phase distribution conveniently. However, when spiral phase plate is employed to induce optical vortex, its construction and fabrication are complex. In contrast, nonspiral phase plate can accomplish optical vortex easily and the plate construction is very simple. In this paper, the focusing properties of optical vortex in Gaussian beam induced by combination of a nonspiral phase plate and a spiral phase are investigated. Some novel focal spots in geometrical focal plane can be obtained and altered.

In the optical system shown in Fig. 1, phase plates provide phase variation in wavefront of an incident laser beam, then the modulated beam with tunable phase is focused through an objective lens. The optical intensity distribution in geometrical focal plane is the research content of this letter. There are two phase plates in the optical path. The phase distribution induced by nonspiral phase plate is $\phi_{\rm p}(y') = C'y'\pi$, and $y' = f\sin(\theta)\cdot\sin(\varphi)$. For small numerical aperture (NA), $\sin(\theta) \approx \theta$, $\theta \in [0, \arcsin(\mathrm{NA})]$ is the convergence angle corresponding to focus point, so

$$\phi_{\rm p}(y') \approx C\theta\sin(\varphi)\pi, \tag{1}$$

where C denotes the phase variation rate, $C = C'f$, $\mathrm{NA} = \sin(\theta_{\max})$ is the NA of the focusing system, (x', y') is the Cartesian coordinate over pupil. Therefore, the phase distribution across the whole pupil is

$$\phi_{\rm p}(\varphi) = \begin{cases} C\theta\sin(\varphi)\pi, & \varphi \in [0, 0.5\pi) \\ 0, & \varphi \in [0.5, 1.5\pi] \\ C\theta\sin(\varphi)\pi, & \varphi \in (1.5, 2\pi) \end{cases}. \tag{2}$$

It can be seen that the nonspiral phase plate introduces phase singularity to the incident beam, as given in Ref. [15].

The phase distribution induced by spiral phase plate is $\phi_{\rm a}(\theta) = D'f\sin(\theta)$, for $\sin(\theta) \approx \theta$ and $\theta \in [0, \arcsin(\mathrm{NA})]$,

$$\phi_{\rm a}(\theta) = D'f\theta = D\theta. \tag{3}$$

Here the spiral phase adjusts the radial phase distribution, and $D = D'f$ denotes the phase variation rate. Therefore, the electric complex amplitude of a vortex Gaussian beam is in the form of

$$E(r,\varphi) = A\exp\left(-\frac{r^2}{\omega^2}\right)\exp\left[i\left(\phi_{\rm p}+\phi_{\rm a}\right)\right], \tag{4}$$

where a is the radius of pupil, r is the radial coordinate, and ω is the radius of incident Gaussian beam. Because $r = f\sin(\theta)$[16], where f is the focal length, Eq. (4) can be rewritten as

$$E(r,\varphi) = A\exp\left(-\frac{[\sin(\theta)/\sin(\theta_{\max})]^2}{(\omega/a)^2}\right)\exp[i(\phi_{\rm p}+\phi_{\rm a})]. \tag{5}$$

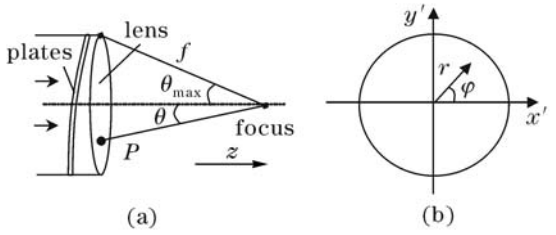

Fig. 1. (a) Optical system and (b) its right view diagraph. Variable θ is the convergence angle related to the point P in pupil plane, $\theta_{\max}$ is its maximum value, and constant f denotes the focal length. r and φ denote cylindrical coordinates. x' and y' are Cartesian coordinates.

1671-7694/2007/050257-03 © 2007 Chinese Optics Letters

For $\mathrm{NA} = \sin(\theta_{\max})$,

$$E(r,\varphi) = A\exp\left(-\frac{\sin^2(\theta)}{\mathrm{NA}^2(\omega/a)^2}\right)\exp[i(\phi_{\mathrm{p}}+\phi_{\mathrm{a}})]. \quad (6)$$

It is assumed that the incident Gaussian beam is linearly polarized along the x' axis. According to vector diffraction theory, and choosing the Herschel apodization function[16], the amplitude of electric field in the focal region can be written as[16,17]

$$\begin{aligned}\vec{E}(\rho,\psi,z) = \frac{i}{\lambda}\iint_{\Omega} E(r,\varphi)\{&[\cos\theta+\sin^2\varphi(1-\cos\theta)]\mathbf{x}\\ &+\cos\varphi\sin\varphi(\cos\theta-1)\mathbf{y}+\cos\varphi\sin\theta\mathbf{z}\}\\ &\times\exp[-ik\rho\sin\theta\cos(\varphi-\psi)]\\ &\times\exp(-ikz\cos\theta)\sin\theta\mathrm{d}\theta\mathrm{d}\varphi, \quad (7)\end{aligned}$$

where $\varphi\in[0,2\pi)$, vectors $\mathbf{x}$, $\mathbf{y}$, and $\mathbf{z}$ are the unit vectors in the x, y, and z directions, respectively. It is clear that the incident beam is depolarized and has three components (E_x, E_y, and E_z) in x, y, and z directions, respectively. The variables ρ, ψ, and z are the cylindrical coordinates of an observation point in the focal region. Based on Eq. (7), the intensity distribution in the focal plane can be computed numerically.

Without loss of generality, it is assumed that $A/\lambda = 1$ and $w = \omega/a = 1$. Optical intensity distributions with different phase variation rates C in the focal plane are computed according to Eq. (7). The effect of parameter D on focal spot is investigated. Figure 2 illustrates the intensity distributions for NA = 0.4, $C = 0$, and different D. It can be seen that for original system without any phase modulation, there is one intensity peak as usual, as shown in Fig. 2(a). Increasing the phase variance parameter D, the intensity peak decreases, and the intensity outside the center peak becomes strong simultaneously. Increasing D continuously, the outside intensity distribution evolves into one intensity ring. When D changes to near 14, the intensity ring becomes very prominent, and its intensity value is bigger than that of the center peak. When the parameter D increases from 14 to 20, the outside intensity ring changes into two intensity rings, then combines back into one intensity ring, as shown in Fig. 2(f).

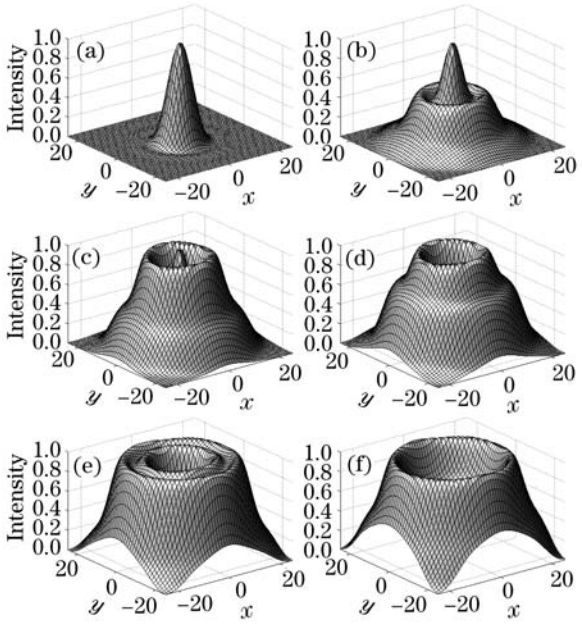

Fig. 2. Intensity distributions for NA = 0.4, $C = 0$, and (a) $D = 0$, (b) $D = 12$, (c) $D = 14$, (d) $D = 16$, (e) $D = 18$, and (f) $D = 20$.

The intensity distributions for NA = 0.4, $C = 5$, and different D are shown in Fig. 3. For $C = 5$ and $D = 0$, there are two intensity peaks. Compared with Fig. 2(a), it can be seen that the parameter C affects the intensity distribution in geometric focal plane considerably. Increasing D, the two intensity peaks rotate in clockwise direction. Simultaneously, the peak shapes also change considerably. The focal evolution for $C = 10$ is also computed and shown in Fig. 4. With increasing the parameter D, the two intensity peaks rotate, and for big D values, the two peaks overlap and form one focal optical intensity curve line.

In order to investigate the effect of initial phase on

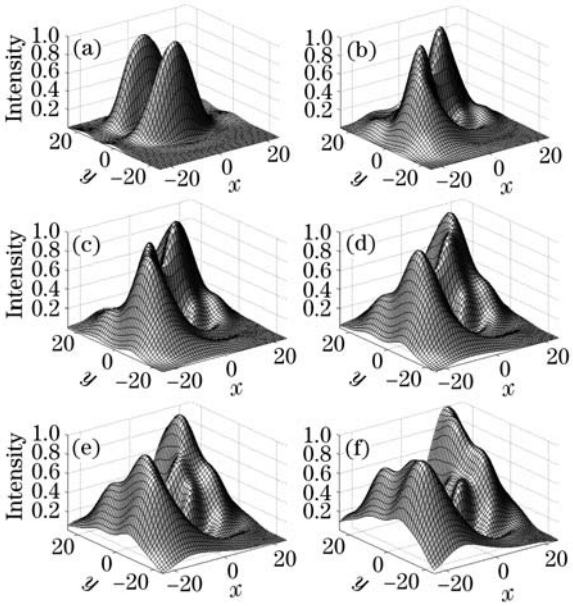

Fig. 3. Intensity distributions for NA = 0.4, $C = 5$, and (a) $D = 0$, (b) $D = 12$, (c) $D = 14$, (d) $D = 16$, (e) $D = 18$, and (f) $D = 20$.

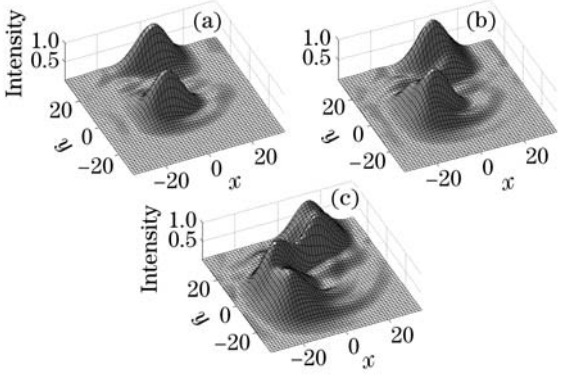

Fig. 4. Intensity distributions for NA = 0.4, $C = 10$, and (a) $D = 6$, (b) $D = 10$, and (c) $D = 16$.

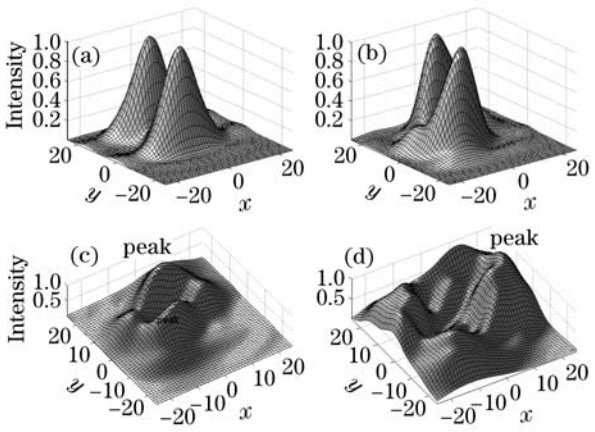

Fig. 5. Intensity distributions for NA = 0.4, $C = 5$, and (a) $D = 0$, (b) $D = 6$, (c) $D = 10$, and (d) $D = 20$.

intensity distributions, the initial phase for nonspiral phase plate is altered as π, so the phase distribution is

$$\phi_{\mathrm{p}}(\varphi) = \begin{cases} C\theta \sin(\varphi)\,\pi + \pi, & \varphi \in [0, 0.5\pi) \\ 0, & \varphi \in [0.5, 1.5\pi] \\ C\theta \sin(\varphi)\,\pi + \pi, & \varphi \in (1.5, 2\pi) \end{cases} . \quad (8)$$

The intensity distributions in focal plane are shown in Fig. 5. There are two intensity peaks, and with increasing D, the two intensity peaks rotate, and then their shapes change considerably. It can be seen that when D approaches to 20, the two peaks evolve into several peaks, and form nearly one ring with dark center focal spot.

Focusing properties of Gaussian beam induced by nonspiral and spiral phase plates are investigated. Intensity distributions in geometrical focal plane show that the parameters of phase plates can alter the intensity distributions considerably and the local dark focal spot may be obtained. The focal spot may evolve into an intensity ring, a two-peak focal spot that may rotate, or an intensity curve line. Therefore, the combination of nonspiral and spiral phase plates can be used to form novel focal spot shapes.

This work was supported by the Science Research Project of Hangzhou Dianzi University (KYS051506021) and the National Natural Science Foundation of China (No. 50574035). X. Gao's e-mail address is gaoxiumin@siom.ac.cn.

References

1. I. V. Basisitiy, M. S. Soskin, and M. V. Vasnetsov, Opt. Commun. **119,** 604 (1995).
2. J. F. Nye and M. V. Berry, Proc. R. Soc. A **336,** 165 (1974).
3. C. T. Law, X. Zhang, and G. A. Swartzlander, Opt. Lett. **25,** 55 (2000).
4. W. M. Lee, X. C. Yuan, and W. C. Cheong, Opt. Lett. **29,** 1796 (2004).
5. K. Ladavac and D. G. Grier, Opt. Express **12,** 1144 (2004).
6. D. Cojoc, V. Garbin, E. Ferrari, L. Businaro, F. Romamato, and E. Di Fabrizio, Microelectron. Eng. **77—78,** 125 (2005).
7. N. R. Heckenberg, R. McDuff, C. P. Smith, and A. G. White, Opt. Lett. **17,** 221 (1992).
8. M. W. Beijersbergen, L. Allen, H. Vanderveen, and J. P. Woerdman, Opt. Commun. **96,** 123 (1993).
9. V. V. Kotlyar, A. A. Almazov, S. N. Khonina, and V. A. Soifer, J. Opt. Soc. Am. A **22,** 849 (2005).
10. X. Gao, Phys. Lett. A **360,** 330 (2006).
11. L. W. Casperson, Opt. Quantum Electron. **8,** 537 (1976).
12. X. Gao, F. Zhou, W. Xu, and F. Gan, Opt. Commun. **239,** 55 (2004).
13. X. Gao, F. Zhou, W. Xu, and F. Gan, Optik **116,** 99 (2005).
14. X. Gao, F. Zhou, F. Zhang, J. T. Yang, W. Xu, and F. Gan, Opt. Eng. **44,** 063001 (2005).
15. G.-H. Kim, J.-H. Jeon, K.-H. Ko, H.-J. Moon, J.-H. Lee, and J.-S. Chang, Appl. Opt. **36,** 8614 (1997).
16. M. Gu, *Advanced Optical Imaging Theory* (Springer, Heidelberg, 2000).
17. D. Ganic, X. Gan, and M. Gu, Opt. Express **11,** 2747 (2003).